

DNA Adsorption by ZnO Nanoparticles near Its Solubility Limit: Implications for DNA Fluorescence Quenching and DNAzyme Activity Assays

Lingzi Ma, Biwu Liu, Po-Jung Jimmy Huang, Xu Zhang, and Juewen Liu*

Department of Chemistry, Waterloo Institute for Nanotechnology

University of Waterloo, Waterloo, Ontario, Canada, N2L 3G1.

*Email: liujw@uwaterloo.ca

Abstract

Zinc oxide (ZnO) is a highly important material, and Zn^{2+} is a key metal ion in biology. ZnO and Zn^{2+} interconvert via dissolution and hydrolysis/condensation. In this work, we explore their interactions with DNA, which is important for biointerface, analytical, and bioinorganic chemistry. Fluorescently labeled DNA oligonucleotides were adsorbed by a low concentration (around 5 $\mu\text{g/mL}$) of ZnO nanoparticles, near the solubility limit. Right after mixing, fluorescence quenching occurred indicating DNA adsorption. Then fluorescence recovered, attributable to ZnO dissolution. The dissolution rate followed $A_5 > T_5 > C_5$. Dissolution was slower with longer DNA. The adsorption affinity was also measured by a displacement assay to be $G_5 > C_5 > T_5 > A_5$, suggesting tightly adsorbed DNA can retard ZnO dissolution. Electrostatic interactions are important for DNA adsorption since ZnO is positively charged at neutral pH, and a high salt concentration inhibits DNA adsorption. Next, in-situ formation of ZnO from Zn^{2+} was studied. First, titrating Zn^{2+} into a fluorescently labeled oligonucleotide at pH 7.5 resulted in an abrupt fluorescence quenching beyond 0.2 mM Zn^{2+} . At pH 6, quenching occurred linearly with Zn^{2+} concentration, suggesting the effect of Zn^{2+} precipitation at pH 7.5. Second, a Zn^{2+} -dependent DNA-cleaving DNAzyme was studied. This DNAzyme was inhibited at higher than 2 mM Zn^{2+} , attributable to Zn^{2+} precipitation and adsorption of the DNAzyme. This paper has established the interplay between DNA, Zn^{2+} , and ZnO. This understanding can avoid misinterpretation of DNA assay results, and adds knowledge to DNA immobilization.

Introduction

Zinc oxide (ZnO) is a wide bandgap semiconductor with very important optical, electronic and catalytic properties.¹ These properties have made ZnO nanoparticles (NPs) a popular choice in developing biosensors, drug delivery vehicles, and bio-imaging agents.²⁻⁷ Over the past few decades, DNA has emerged as a programmable and functional molecule in analytical chemistry,⁸⁻¹² nanotechnology and materials science.¹³ Attaching DNA to ZnO adds molecular recognition function to the particle, enables directed assembly, and facilitates device incorporation. To reach its full potential, the surface science of DNA adsorption by ZnO needs to be understood. A few previous studies touched upon this topic. For example, even low concentrations of ZnO NPs can damage DNA.¹⁴⁻¹⁵ Direct interfacing ZnO with nucleic acids was demonstrated with long double-stranded DNA.¹⁶ DNA has also been used as a template to direct the growth of ZnO NPs.¹⁷⁻¹⁸ By screening random DNA sequences, it was reported that the T₃₀ DNA (a DNA with 30 thymine bases) has a strong affinity for ZnO.¹⁹

A related aspect is the interaction between Zn²⁺ ions and DNA. Zinc is one of the most important transition metals in biology, serving as a metal cofactor in many protein enzymes.²⁰⁻²¹ At the same time, Zn²⁺ is also frequently used for assisting DNAzyme catalysis. DNAzymes are DNA-based catalysts.²²⁻²⁵ Zn²⁺-dependent RNA-cleaving,²⁶⁻²⁷ DNA-cleaving,²⁸⁻²⁹ and DNA-ligating DNAzymes have been reported.³⁰

We introduce ZnO and Zn²⁺ together because the transition from Zn²⁺ to ZnO or Zn(OH)₂ takes place at physiological pH with sub-mM Zn²⁺.³¹ In many cases, Zn²⁺ is used at ~1 mM with DNA, making Zn²⁺ hydrolysis/precipitation a valid concern. However, this aspect has been rarely considered, and we believe it has a profound influence. In this work, we start with a basic surface science analysis of the adsorption and desorption of DNA oligonucleotides by ZnO NPs. We then

relate our observations to Zn²⁺-induced fluorescence quenching and DNAzyme assays, which are significantly influenced by the hydrolysis of Zn²⁺.

Materials and Methods

Chemicals. The DNA samples used in this work were from Integrated DNA Technologies (IDT, Coralville, IA). The DNA sequences are listed in Table 1. Zinc oxide NPs (catalog number: 721077-100G) and 8-hydroxy-5-quinolinesulfonic acid (HQS) were from Sigma-Aldrich. Sodium chloride, sodium carbonate, zinc chloride, 2-(N-morpholino) ethanesulfonic acid (MES), 4-(2-hydroxyethyl) piperazine-1-ethanesulfonate (HEPES), and the nucleosides were from Mandel Scientific (Guelph, ON). Milli-Q water was used to prepare all the buffers and solutions.

Table 1. DNA sequences and modification used in this work. FAM = carboxyfluorescein; AF = Alexa Fluor 488.

DNA names	sequences (5' → 3') and modifications
FAM-A ₅	FAM-AAAAA
FAM-T ₅	FAM-TTTTT
FAM-C ₅	FAM-CCCCC
FAM-G ₅	FAM-GGGGG
FAM-A ₁₅	FAM-AAAAAAAAAAAAAAAAA
FAM-A ₃₀	FAM-AAAAAAAAAAAAAAAAAAAAAAAAAAAAAAAAA
FAM-A ₄₅	FAM-AAA
A ₅	AAAAA
T ₅	TTTTT

C ₅	CCCCC
G ₅	GGGGG
AF-DNA	TCACAGATGCGT-AF
I-R3 Substrate	CGTTCGCCTCATGACGTTGAAGGATCCAGACT-FAM
I-R3 DNAzyme	AGTCTGGATCTAGTTGAGCTGTCATGAGGCGAACG

DLS, XRD and TEM. The hydrodynamic size and ζ -potential of ZnO NPs (100 $\mu\text{g}/\text{mL}$) were measured by dynamic light scattering (DLS) using a Zetasizer Nano ZS90 (Malvern). To obtain pH-dependent ζ -potential, NaOH was added to adjust the pH value of ZnO dispersion in Milli-Q water (pH 7.5 to 11) at 25 °C. Powder X-ray diffraction was performed using a PANalytical Empyrean X-ray diffractometer with Cu-K α radiation ($\lambda=1.78901 \text{ \AA}$). Transmission electron microscopy (TEM) and high-resolution transmission electron microscopy (HRTEM) were performed on a Philips CM10 and a Zeiss Libra 200MC microscope, respectively. The TEM samples were prepared by dropping ZnO dispersion (20 $\mu\text{g}/\text{mL}$) on a copper grid followed by drying in air.

DNA adsorption assays. To study DNA adsorption kinetics, 1 μL FAM-A₅ DNA (1 μM) stock solution was dissolved into 94 μL of HEPES buffer (10 mM, pH 7.5) in a half-area black 96-well plate (final DNA concentration of 10 nM). The initial fluorescence of FAM-DNA was monitored for 3-5 min (excitation at 485 nm, emission at 535 nm) using a microplate reader (Infinite F200Pro, Tecan) prior to a quick addition and mixing of 5 μL of 100 $\mu\text{g}/\text{mL}$ ZnO NPs (final concentration of 5 $\mu\text{g}/\text{mL}$). Afterwards, the adsorption kinetics was tracked for 30 min. To further study the effect of DNA length and sequence, FAM-labeled C₅, T₅, G₅, A₁₅, A₃₀ and A₄₅ were respectively

tested. The same procedure was applied at different pH values (10 mM, HEPES buffer for pH 7, 7.5, 7.8, and 8, and carbonate buffer for pH 10). The function of ionic strength was studied by varying the concentration of NaCl (50, 150, or 300 mM). To study the effect of ZnO concentration, FAM-A₅ (10 nM) was mixed with various concentrations of ZnO NPs (0, 1, 2, 3, 5, 7, 10, 15, 20, or 25 µg/mL). Note that the volume of ZnO NPs was kept smaller than 5 µL for each addition. For the displacement experiment, 15 µg/mL ZnO NPs were mixed with FAM-A₅ (10 nM). Then 100 nM non-labeled DNA was added to displace the adsorbed FAM-A₅. Typical measurements were done in triplicate to obtain standard deviations.

Fluorescence quenching assays. First, 10 nM FAM-A₅ or AF-DNA was dissolved in 10 mM HEPES (pH 7.5) or MES buffer (pH 6.0) containing NaCl (0 or 1 M). Then, ZnCl₂ was gradually titrated to a final Zn²⁺ concentration of 1 mM. The fluorescence was measured at 5 min after each addition of ZnCl₂.

HQS assays. A solution of 2 mM HQS was prepared in HEPES buffer (10 mM, pH 7.5). A standard curve was built by measuring the fluorescence of HQS in the presence of a series concentrations of ZnCl₂ (excitation at 393 nm, emission at 521 nm) using the plate reader. The Zn²⁺ produced by the dissolution of ZnO NPs was next studied by adding various concentrations of ZnO NPs to 2 mM HQS in the same buffer.

DNAzyme cleavage assays. A 1 M ZnCl₂ stock solution was diluted in 50 mM HEPES buffer (pH 7.6) to prepare a series of ZnCl₂ concentrations. The pH of each ZnCl₂ solution was carefully adjusted to 7.6. For each sample, two tests were made. For the first test, the samples were directly used even though the high zinc concentration samples were precipitated. For the second test, the samples were centrifuged at 15000 rpm for 10 min, and the supernatant containing the soluble Zn²⁺ was transferred to another tube and used. The stock DNAzyme complex was prepared by annealing

the substrate (20 μM) and enzyme (30 μM) in HEPES buffer (50 mM, pH 7.6). The cleavage activity assays were performed with a final concentration of 2.86 μM DNAzyme complex in the presence of different ZnCl_2 concentrations (0, 0.1, 0.2, 0.5, 1, 2, 5, or 10 mM). After 1 h of incubation, the reactions were quenched with 8 M urea. The cleavage products were separated on a 15% denaturing PAGE gel and documented using a ChemiDoc MP imaging system (Bio-Rad).

Results and Discussion

An intriguing DNA adsorption profile. Our ZnO NPs have an average size of ~ 20 nm as indicated by both the vendor and TEM (Figure 1A). The particles are irregular in morphology and moderately aggregated. Its hydrodynamic size is ~ 46 nm from dynamic light scattering (Figure 1B), consistent with the TEM observation. Our ZnO has a hexagonal wurtzite nanocrystalline structure as indicated by XRD (Figure 1C). High resolution TEM also confirmed the crystallinity of the particles (Figure 1D).

Fluorescently labeled DNA oligonucleotides are excellent probes for studying DNA adsorption. In this study, we started with a FAM-labeled A_5 DNA. The initial fluorescence of the free DNA was monitored for 3 min before a small volume of ZnO NPs was added to achieve a final concentration of 5 $\mu\text{g/mL}$ ZnO. Immediately following ZnO addition, the fluorescence dropped by over 80% (Figure 2A, red trace), suggesting very fast DNA adsorption. ZnO has a wide band gap of 3.37 eV, and fluorescence quenching by ZnO is likely due to electron transfer from the excited fluorophore to the conduction band of ZnO. This mechanism was reported for TiO_2 , which has a similar band gap of 3.2 eV.³²

Interestingly, after the initial drop, the fluorescence gradually recovered to the original value over ~ 5 min. We previously studied DNA adsorption³³ by metal NPs,³³ other metal oxides,³⁴⁻

³⁷ and graphene oxide.³⁸ This is the first time to observe such fluorescence recovery. Therefore, we explored it further.

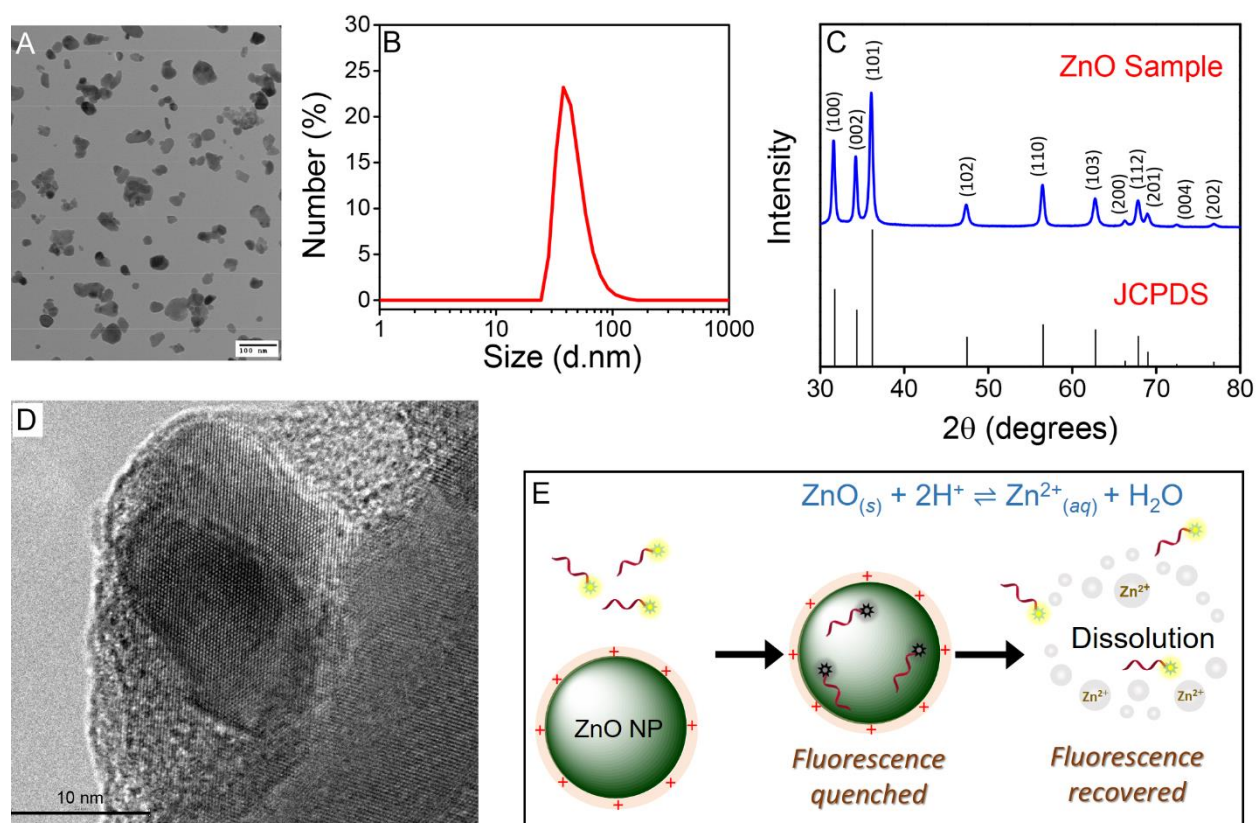


Figure 1. A TEM (A) and high resolution TEM (D) micrograph of the ZnO NPs used in this work. (B) The dynamic light scattering (DLS) spectrum of the ZnO NPs (0.1 mg/mL in water). (C) Powder XRD spectrum of the ZnO NPs and the standard spectrum of hexagonal wurtzite ZnO. (D) A scheme of DNA/ZnO interaction near its solubility limit. DNA adsorption resulted in quenched fluorescence. If the ZnO NP concentration is low, it may dissolve and release the adsorbed DNA.

Effect of DNA sequence and length. To understand this fluorescence recovery, we next studied the effect of DNA length using poly-A DNA. FAM-A₁₅ showed a similar degree of initial quenching, while the subsequent recovery was much slower (Figure 2A, blue trace). The degree of quenching substantially decreased with the A₃₀ and A₄₅ DNAs, and their fluorescence recovery

was even less. The decreased adsorption by longer DNA can be explained by the saturation of ZnO surface since a longer DNA needs more surface footprint. Longer DNA may also have less quenching since its fluorophore is likely to be farther away from the ZnO surface. Note that surface quenching is often distance-dependent.^{32,39-40} To better compare the kinetics of fluorescence recovery, we normalized the initial fluorescence value based on the time point right after ZnO addition (Figure 2B). This plot confirms the rate of fluorescence recovery is inversely correlated to the length of DNA.

Considering that FAM is a relatively large label with a size similar to a nucleotide, it is important to make sure that this label is not adsorbed by ZnO. Otherwise, it may cause artifacts in our data interpretation. To test this, we prepared a 10 nM free fluorescein solution (the same concentration as the above DNA probes) and added increasing concentrations of ZnO NPs (Figure 2C). No fluorescence quenching was observed suggesting the lack of adsorption with up to 50 $\mu\text{g/mL}$ of ZnO. Therefore, the above fluorescence quenching was due to DNA adsorption instead of direct fluorophore adsorption.

Since the shortest A₅ DNA showed the fastest fluorescence recovery, we next employed other 5-mer DNA homopolymers to study the effect of DNA sequence (Figure 2D). Among these, FAM-T₅ also showed significant quenching followed by full recovery similar to that for FAM-A₅. Interestingly, FAM-C₅ recovered very slowly. Since guanine is a strong fluorescence quencher, FAM-G₅ had very weak initial fluorescence. As such, we did not observe much further fluorescence drop after mixing FAM-G₅ with ZnO. Therefore, we cannot judge the G₅ DNA adsorption by ZnO at this moment.

From previous studies on biopolymer adsorption,⁴¹ such fluorescence recovery after DNA adsorption is usually interpreted as an expansion of the flexible DNA on surface following the

initial adsorption, pushing weakly adsorbed DNAs off the surface. However, this cannot explain the full recovery of fluorescence (all DNA desorbed) in our system. We propose that the fluorescence recovery is due to dissolution of ZnO NPs when the particle concentration is low (reaching the solubility limit). If so, our results suggest that adsorption of certain DNA (e.g. C₅ and long poly-A DNA) might retard ZnO dissolution, control its solubility, and even promote the growth of ZnO nanocrystals. Figure 1E shows the scheme of DNA adsorption on ZnO NPs followed by NP dissolution.

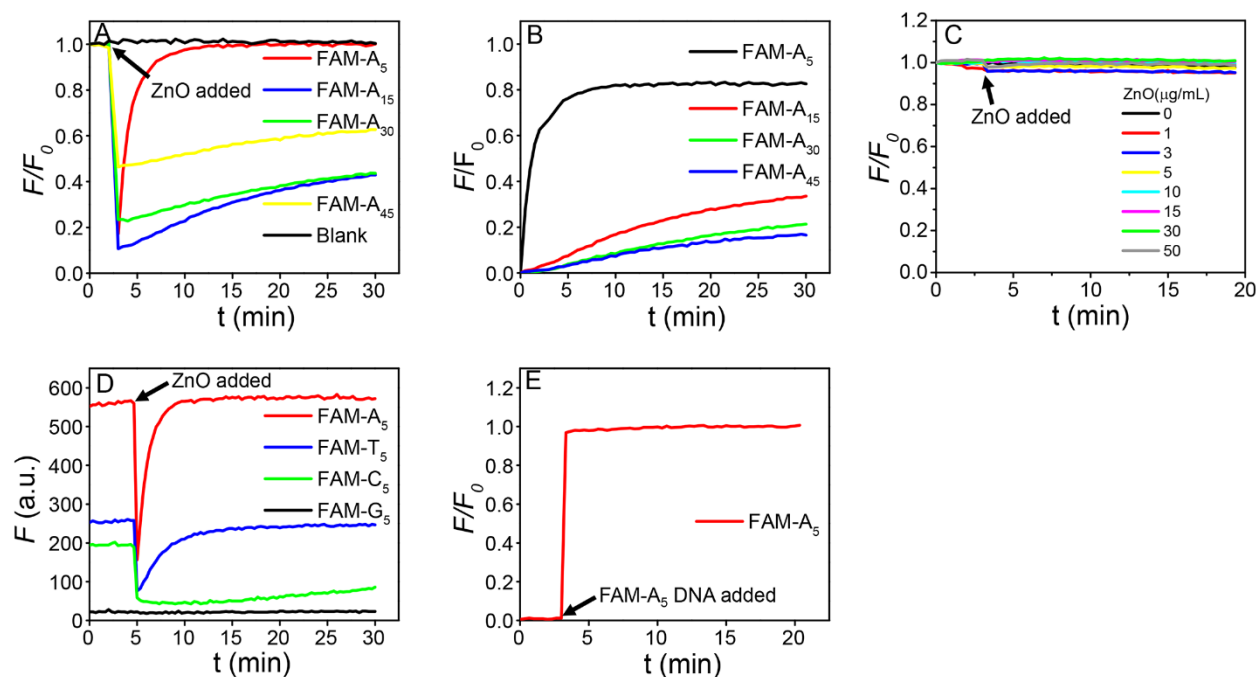


Figure 2. Adsorption of FAM-labeled DNA by ZnO NPs. (A) 5 µg/mL ZnO NPs were mixed with 10 nM poly-A of different lengths. (B) Normalized fluorescence intensity from the recovery stage in (A) after adding ZnO. Fluorescence recovered more slowly with longer DNA. (C) Fluorescence intensity of 10 nM free fluorescein (50 mM HEPES, pH 7.5) and after adding various concentrations of ZnO NPs. (D) Adsorption kinetics of different DNA sequences by 5 µg/mL of ZnO NPs. (E) A dispersion of ZnO NPs (5 µg/mL) was first prepared followed by adding FAM-

A₅. The lack of fluorescence quenching indicates no adsorption (ZnO already fully dissolved before DNA addition).

Effect of ZnO concentration. To test our hypothesis on ZnO dissolution, we switched the order of sample addition (Figure 2E). First, 5 µg/mL of ZnO was added to the buffer, and FAM-A₅ was added 3 min later. In this case, we did not observe any fluorescence drop, suggesting that the ZnO NPs had fully dissolved before the DNA addition. To quantitatively understand the effect of ZnO concentration, we fixed the FAM-A₅ DNA at 10 nM, and gradually increased the ZnO concentration (Figure 3A). With just 1 µg/mL ZnO, no adsorption phase was detected, suggesting a very rapid dissolution. As more ZnO was added, more adsorption took place followed by slower fluorescence recovery until 15 µg/mL of ZnO was reached. At that point, no fluorescence recovery took place, indicating full DNA adsorption. At this moment, sufficient ZnO remained in the solid phase to adsorb all the DNA.

This series of adsorption kinetics in Figure 3A, in turn, delineate the solubility profile of ZnO NPs in our buffer (10 mM HEPES, pH 7.5, room temperature). Below 5 µg/mL of ZnO, the fluorescence fully recovered to the initial intensity, suggesting a complete dissolution of ZnO NPs. Above that concentration, a portion of ZnO remained in the NP form during the time frame of 25 min. From the literature, the solubility of ZnO NPs (~30 nm diameter) was 16 µg/mL as measured by equilibrium dialysis under similar conditions (2 mM PIPES, pH 7.5, 24 °C).⁴² This is in good agreement with our DNA probing data, where full DNA adsorption took place at 15 µg/mL of ZnO or higher.

The concentration of Zn²⁺ is 180 µM after fully dissolving 15 µg/mL of ZnO. This concentration is highly relevant to the application of Zn²⁺ in nucleic acids chemistry. In other

words, we need to consider the formation of ZnO or Zn(OH)₂ by adding free Zn²⁺ above this concentration, and dissolution of the ZnO NPs below this concentration. We hypothesize that stable adsorption can be achieved also for other DNA sequences if we raise the ZnO concentration to 15 µg/mL. Indeed, we observed stable adsorption with similarly strong fluorescence quenching for all the DNA lengths (Figure 3B), and DNA sequences (Figure 3C) tested. From here on, 15 µg/mL ZnO was used to avoid the dissolution effect.

To understand the zinc species after dissolving ZnO, we used 8-hydroxy-5-quinolinesulfonic acid (HQS) as a fluorescent Zn²⁺ probe.⁴³ Free HQS (2 mM) is almost non-fluorescent (Figure 3D, black trace). After adding 75 µM Zn²⁺, a strong emission peak at 521 nm was obtained. After adding 5 µg/mL of ZnO to the same concentration of HQS, a similar emission peak was observed, suggesting dissolution of ZnO to free Zn²⁺ ions. We further made a calibration curve using various concentrations of Zn²⁺, which was used to predict the Zn²⁺ from dissolved ZnO. The predicted values agree well with the calculated values, confirming the full dissolution of ZnO (1 to 10 µg/mL) to Zn²⁺ (Figure 3E).

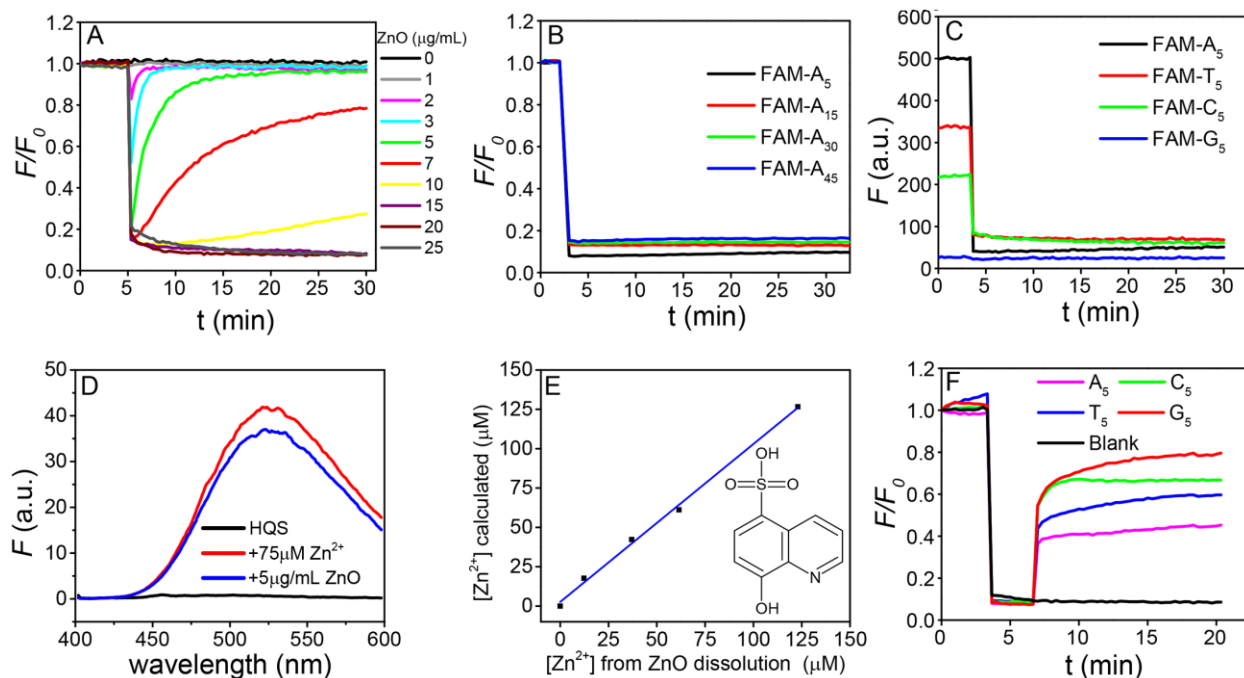


Figure 3. (A) FAM-A₅ DNA (10 nM) adsorption by various concentrations of ZnO NPs at pH 7.5. Fluorescence quenching kinetics by adding 15 µg/mL ZnO NPs to (B) poly-A DNAs of different lengths and to (C) 5-mer DNAs of different sequences. Fluorescence spectra of 2 mM HQS and its mixture with 75 µg/mL Zn²⁺ or with 5 µg/mL of ZnO. (E) Correlation of calculated Zn²⁺ from fully dissolved ZnO and the measured value using the HQS sensor. Inset: the structure of HQS. (F) Displacement experiment performed by adding non-labeled A₅, T₅, C₅, and G₅ to the adsorbed FAM-A₅.

Displacement of adsorbed DNA. After achieving stable DNA adsorption, we further studied the relative adsorption affinity of different DNA using a displacement assay. First, 15 µg/mL of ZnO NPs was mixed with 10 nM FAM-A₅ to achieve full DNA adsorption. Then a 10-fold excess of non-labeled DNA (A₅, T₅, C₅ or G₅, 100 nM each) was respectively added. The normalized kinetic traces of fluorescence change are shown in Figure 3F. In this case, G₅ gave the highest fluorescence

recovery suggesting it displaced the largest amount (~80%) of adsorbed FAM-A₅. It is interesting to note that adding 10-fold excess of A₅ only recovered the fluorescence by ~40%. The incomplete displacement is partially attributed to that the original ZnO surface was not saturated by FAM-A₅. Therefore, a fraction of the added DNA was directly adsorbed on the particle surface without displacing a FAM-A₅ DNA. All the samples had a fast displacement in the first minute followed by a slower kinetic phase. This suggests that a fraction of the FAM-A₅ DNA was initially weakly adsorbed and easily displaced. The slower phase can be attributed to the displacement of more tightly adsorbed DNA. As the surface became more densely packed by DNA, further displacement might become even slower due to the electrostatic repulsion between incoming DNA and the DNA on surface. This experiment indicates that the adsorption affinity of DNA follows the following order: G₅>C₅>T₅>A₅. Therefore, the previous lack of fluorescence quenching upon mixing FAM-G₅ with ZnO is due to the very low initial fluorescence of this DNA instead of a lack of adsorption.

By combining this adsorption affinity data and the fluorescence recovery data in Figure 2D, we conclude that a more stably adsorbed DNA can better retard ZnO dissolution. In a previous theoretical study, it was hypothesized that ZnO NPs form site-specific and stable complexes with nucleobases, which might explain our observation of different DNA sequences.⁴⁴ Morse and co-workers performed a DNA aptamer selection against ZnO and found that the T₃₀ DNA was the most in the final library (1.97%). They concluded that T₃₀ might be a DNA aptamer for ZnO.¹⁹ Our study, using much shorter DNA, indicates that while T₅ binds ZnO stronger than A₅, it is much weaker than C₅ and G₅.

Adsorption mechanism. The above results indicate that ZnO can quickly adsorb DNA. DNA adsorption is a function of its length and sequence. In addition, ZnO has a relatively high solubility at neutral pH. Next, we studied the mechanism of DNA adsorption. Since DNA is a polyanion, we

measured the ζ -potential of ZnO NPs as a function of pH (Figure 4A). At pH near 7.5, ZnO is positively charged. Its surface charge decreases almost linearly with increasing pH, and the point of zero charge is pH 8.8. The reason for pH-dependent surface charge inversion can be explained by the protonation of the surface $-\text{OH}$ groups on ZnO when dispersed in water. If the ZnO surface is covered by $-\text{OH}$ groups, the charge is neutral (Figure 4B). At higher pH, this group deprotonates to produce $-\text{O}^-$, which gives a negative charge; while at lower pH, it protonates to yield positively charged $-\text{OH}_2^+$. Therefore, in the above assay condition of pH 7.5, ZnO is positively charged. This explains the fast DNA adsorption kinetics due to a strong electrostatic interaction. We further tested the effect of pH on DNA adsorption (Figure 4C). For all these samples, more initial fluorescence quenching occurred at higher pH, and higher pH also resulted in slower fluorescence recovery. The dissolution of ZnO can be written as $\text{ZnO} + \text{H}_2\text{O} \rightleftharpoons \text{Zn}^{2+} + 2\text{OH}^-$. At higher pH, the equilibrium favors ZnO formation and DNA adsorption, which explains the pH effect.

At even higher pH (e.g. pH 10) passing the point of zero charge, the ZnO surface became negatively charged, and DNA adsorption is also inhibited (Figure 4D, black trace). Therefore, DNA adsorption by ZnO is affected by two factors: dissolution and surface charge. At pH lower than 8.8 with a low ZnO concentration (e.g. lower than the solubility limit), while DNA can be quickly adsorbed, DNA cannot be stably adsorbed due to ZnO dissolution. If the ZnO concentration is high and not fully dissolved, then effective adsorption can be achieved based on electrostatic attraction. In the range of pH lower than 8.8, if ZnO is not fully dissolved, lower pH favors DNA adsorption. At even higher pH passing pH 8.8 (e.g. pH 10), while dissolution problem is more alleviated, the ZnO surface becomes negatively charged and DNA cannot be adsorbed.

Ionic strength can also modulate electrostatic interactions. We carried out all the above studies in the absence of salt. Here, we also measured the adsorption by adding salt. At pH 7.5,

adsorption of the FAM-A₅ DNA significantly decreased with 50 mM NaCl, and was fully inhibited with 150 mM or higher NaCl (Figure 4E), which can be explained by the charge screening effect of NaCl. The pH and salt dependent studies confirmed the importance of electrostatic interactions in DNA adsorption by ZnO NPs. It is interesting to note that at pH 10, no DNA adsorption was observed regardless of the NaCl concentration (Figure 4D). This is likely due to that even after screening the charge repulsion, the attraction force is still very weak (e.g. the surface of ZnO covered by $-O^-$ and cannot achieve stable DNA adsorption).

In addition to testing the charge interaction, we next probe specific binding between the DNA and ZnO. DNA has a negatively charged phosphate that may interact with the Zn centers on the ZnO surface, and the DNA bases may also contribute to the adsorption through coordination interactions. To test this, we first adsorbed 100 nM FAM-A₁₅ DNA on 30 μ g/mL ZnO in HEPES buffer (10 mM, pH 7.5, 150 mM NaCl). The high salt concentration was used to screen the electrostatic interaction between DNA and ZnO NPs. Then, free phosphate and various nucleosides were respectively added to displace the adsorbed DNA (Figure 4F). Strong fluorescence signal was observed only in the presence of phosphate, suggesting that phosphate can displace the adsorbed DNA. This also indicates a specific binding between phosphate and ZnO, which may also occur in the DNA. Although the C₅ DNA can stabilize ZnO NPs against dissolution, free cytidine failed to bring any fluorescence enhancement. Therefore, if the bases are playing a role, it must be secondary. On the other hand, the base coordination, although weak on the individual base level, might still play a role when a few bases can act together to form polyvalent binding.

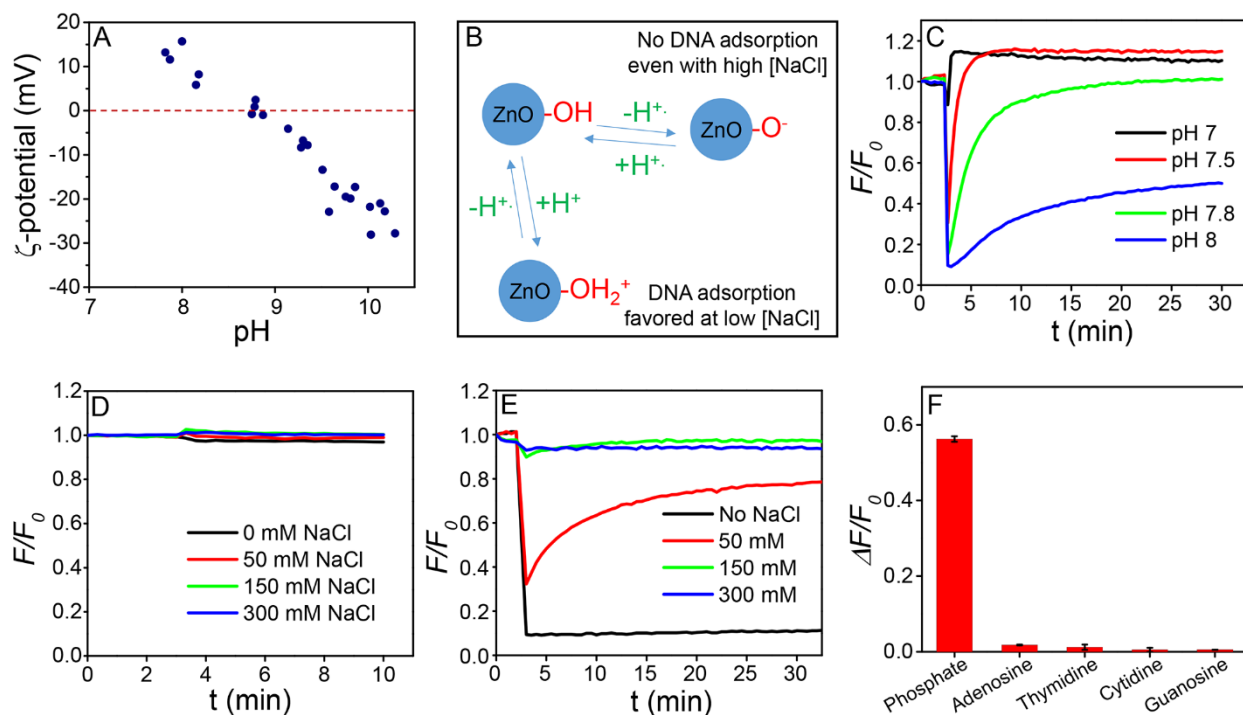


Figure 4. (A) The ζ -potential of ZnO NPs as a function of pH. (B) A scheme showing the origin of surface charge on ZnO NPs as a function of pH. FAM-A₅ DNA adsorption kinetics as a function of (C) pH without salt and (E) salt concentration at pH 7.5. (D) FAM-A₅ DNA adsorption at pH 10 in various NaCl concentrations. (F) Displacement of the FAM-A₁₅ DNA by various nucleosides and free phosphate (1 mM each).

Implications for DNA fluorescence quenching assays. The above studies focused on the fundamental surface science of ZnO, and highlighted the effect of ZnO dissolution. This understanding is useful for immobilization of DNA on ZnO. Next, we focus on the reverse reaction: *in-situ* (and often unintended) production of ZnO species. Many transition metals can quench fluorescence through the energy or electron transfer.⁴⁵⁻⁴⁷ Hence, quenching induced by adding these metals is often interpreted as such. Since we know that ZnO can quench fluorescence as well, we want to explore this front.

The fluorescence intensity of FAM-A₅ was measured at pH 7.5 as a function of ZnCl₂ concentration. This experiment was performed in the presence of either 0 or 1 M NaCl. For all the samples, no obvious fluorescence quenching was observed below 100 $\mu\text{M Zn}^{2+}$ (Figure 5A). Without NaCl, an abrupt quenching occurred at 200 $\mu\text{M Zn}^{2+}$ and above. This quenching certainly cannot be explained by Zn^{2+} acting either as a dynamic or static quencher. The quenching is more consistent with a phase transition to form ZnO or Zn(OH)₂ adsorbing DNA. With 1 M NaCl, we did not observe quenching that can be explained by charge screening hindering DNA adsorption. Note that, 200 $\mu\text{M Zn}^{2+}$ can convert to 17 $\mu\text{g/mL}$ of ZnO. This is consistent with the solubility limit of ZnO under our experimental conditions. Therefore, the adsorption of DNA on the *in-situ* formed ZnO NPs might be the most crucial factor responsible for the abrupt fluorescence quenching. Without considering ZnO formation, it might have been mistakenly attributed to fluorescence quenching by Zn^{2+} .

To further confirm the effective species in the quenching phenomena, we performed the same assay at a lower pH. Since FAM is pH sensitive, an AF-labeled DNA was used in this case. The solubility of Zn^{2+} is a strong function of pH and ZnO formation is disfavored at lower pH. At pH 6.0 (Figure 5B), we only observed a gradual Zn^{2+} -concentration dependent quenching in the absence of NaCl. This type of response is more likely due to free Zn^{2+} ions, which can exist at acidic pH. Interestingly, with 1 M NaCl, Zn^{2+} still failed to quench the fluorescence at pH 6. This is likely due to NaCl screening the Zn^{2+} and DNA interaction. The abnormal DNA fluorescence change at pH 8.6 by $>1 \text{ mM Zn}^{2+}$ was also observed in a fluorescent resonance energy transfer study by Clegg and co-workers,⁴⁸ and it was attributed to aggregation of DNA. With our data here, it is more likely to be caused by DNA aggregation due to precipitated Zn^{2+} .

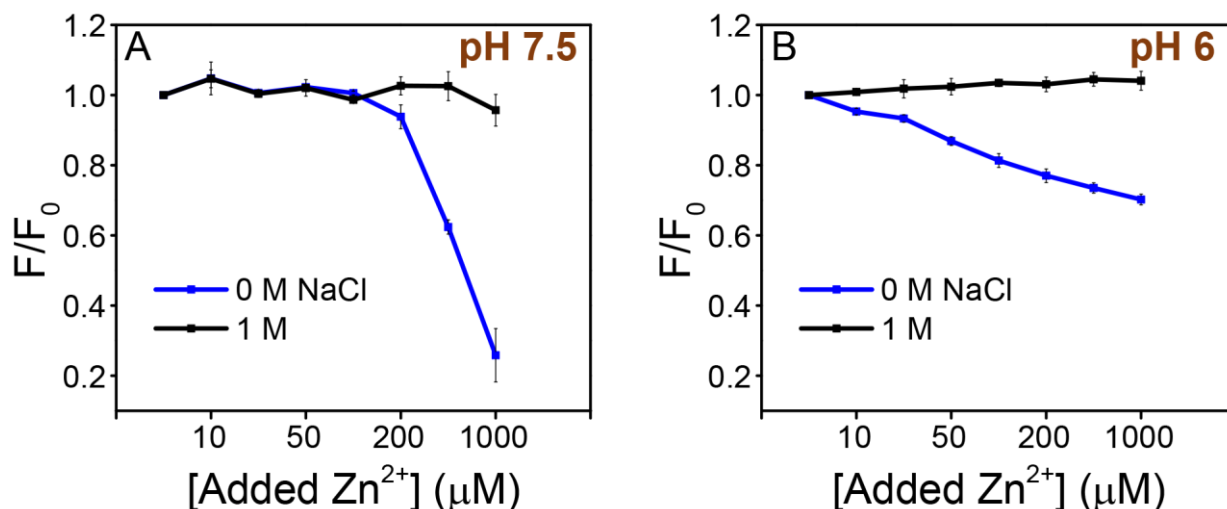


Figure 5. Normalized fluorescence of (A) 10 nM FAM-A₅ in 10 mM pH 7.5 HEPES buffer and (B) 10 nM AF-labeled DNA in pH 6 MES buffer as a function of Zn²⁺ concentration (with 0 or 1M NaCl).

Effect on DNAzyme cleavage assay. In addition to fluorescence quenching, Zn²⁺ precipitation may affect other aspects of DNA assays as well. Here, we further studied a DNAzyme cleavage reaction. Recently, Breaker and co-workers isolated a Zn²⁺-dependent DNAzyme named I-R3.²⁹ With 2 min reaction time, cleavage was observed only with 1-5 mM Zn²⁺ with 2 mM Zn²⁺ being the most efficient. Barely any cleavage was observed with below 0.2 mM Zn²⁺. Therefore, the enzyme activity does not increase linearly in the low Zn²⁺ concentration region. At the same time, the enzyme activity peaks at pH ~7 and drops rapidly on either side. Since the relevant Zn²⁺ concentrations and pH of this DNAzyme are related to the range studied in this work, we used this DNAzyme as a model system to study the effect of Zn²⁺ precipitation. For example, precipitated zinc species may interfere with the reaction by adsorbing DNA, and thereby inhibit the cleavage reaction. We designed a trans-cleaving DNAzyme complex (Figure 6A) with the same core

sequences. This complex contains a substrate strand shown in red with a FAM label and an enzyme strand in black. We followed the cleavage of this DNAzyme with 1 mM Zn²⁺. A significant cleavage was observed at 2 min and saturated cleavage was reached after 20 min (Figure S1), confirming the activity of this DNAzyme.

To minimize the pH difference due to the added ZnCl₂, which is acidic, various concentrations of ZnCl₂ were first mixed with the HEPES buffer followed by a precise pH adjustment to 7.6. During this process, visible precipitants were noticed at 2.0 mM Zn²⁺ and above. Therefore, for these samples, the free Zn²⁺ concentration must be lower than the intended value. We then carried out the cleavage reactions with these Zn²⁺ samples. As shown in Figure 6B, the cleavage activity was observed from 0.2 to 2 mM Zn²⁺, with 0.5 mM Zn²⁺ being optimal. Beyond 2 mM, little cleavage was observed, consistent with the literature report.

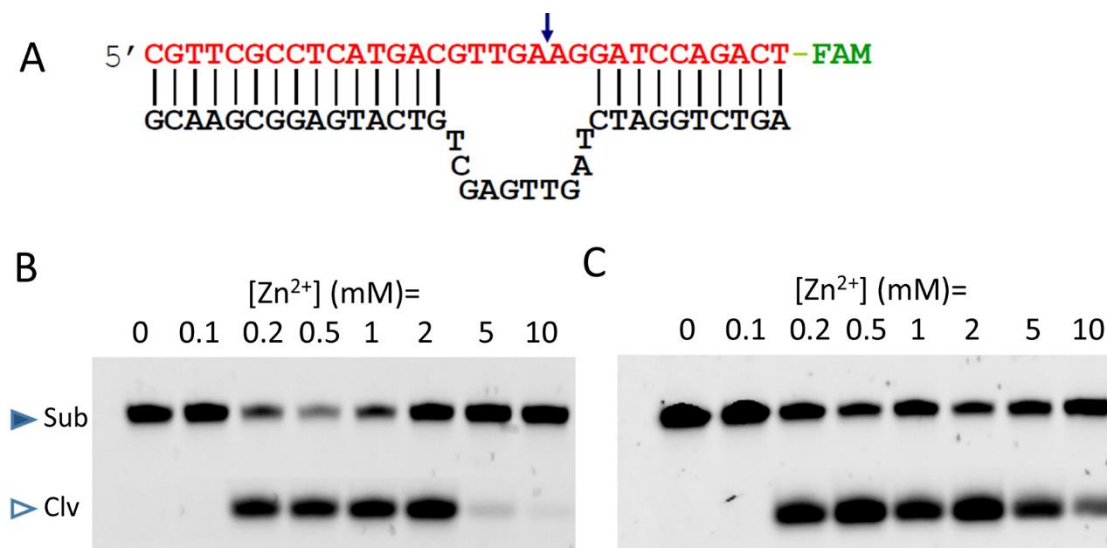


Figure 6. (A) The Zn²⁺-dependent DNA-cleaving I-R3 DNAzyme used in this work, where the substrate strand is labeled with a FAM fluorophore on its 3'-end, and the cleavage site is indicated by the arrowhead. Gel images showing the DNAzyme activity as a function of Zn²⁺ concentration

using the mixture (B) or the supernatant fraction (C). The upper band is the uncleaved substrate and the lower one is the cleaved FAM-bearing fragment.

Then we centrifuged all the Zn^{2+} samples, and the supernatants were transferred to perform the same cleavage reaction. In this case, we observed cleavage even with 10 mM Zn^{2+} (Figure 6C). This experiment indicates enhanced DNAzyme activity after removal of the precipitates. Therefore, the lack of DNAzyme activity for the high Zn^{2+} samples in Figure 6B is due to the inhibition from the precipitants, which is likely to be caused by its adsorption of the DNAzyme.

Next, we tested whether salt can alleviate the inhibition effect since salt can weaken DNA adsorption by ZnO due to charge screening. The assay was performed with 10 mM Zn^{2+} and cleavage was indeed observed in the presence of 500 mM and 1 M NaCl (Figure S2). A high salt concentration was used in the original assays by the Breaker group, and the effect of Zn^{2+} precipitation was less of a concern in their experiments. We used this DNAzyme as an example to articulate the potential artifacts that might be caused by the low solubility of Zn^{2+} .

Many DNAzymes use Mg^{2+} as a metal cofactor, which is highly soluble compared to other metal ions at neutral pH (e.g. up to 50 mM or higher Mg^{2+} can be used).⁴⁹ Many transition metals including Pb^{2+} , UO_2^{2+} , and lanthanides are active at much lower concentrations (e.g. low μM or even nM).⁵⁰⁻⁵² Therefore, their concern of forming bulk precipitation is also lessened. Zn^{2+} , however, is typically used at relatively higher concentrations (high μM to low mM) at neutral pH, making its hydrolysis and precipitation particularly important.

Conclusions

In summary, we studied the interaction between DNA and zinc from two aspects. First, the adsorption of DNA by ZnO NPs was measured as a function of salt, pH, and DNA sequence and

length. We paid particular attention to the dissolution of ZnO by using a low particle concentration. The electrostatic interaction between negatively charged DNA and positively charged ZnO NPs produced fast adsorption kinetics. The negatively charged phosphate backbone of DNA is mainly responsible for adsorption, and DNA bases are likely to contribute to adsorption as well. At low ZnO concentrations (<15 $\mu\text{g/mL}$), DNA adsorption is accompanied by desorption due to ZnO dissolution. Tightly adsorbing DNA, such as poly-C, can retard ZnO dissolution. Second, we started with free Zn^{2+} ions at high pH (e.g. pH 7.5 above), where high micromolar Zn^{2+} can precipitate, and such precipitants can adsorb DNA. The consequence of such adsorption is substantiated in two DNA-based assays involving Zn^{2+} : fluorescence quenching and DNAzyme cleavage. In both cases, the experimental observations can be explained by DNA adsorption. For the many materials studied for DNA adsorption so far, this dissolution and precipitation happens only with zinc, which is a highly important metal for interfacing with nucleic acids. Other than the fundamental insights into the ZnO/DNA interface, this work is valuable for interpreting related experimental data on Zn^{2+} -based nucleic acids research.

Supporting Information

The Supporting Information is available free of charge on the ACS Publications website at DOI:

10.1021/acs.langmuir.xxxxxxx

Additional DNAzyme assay data (PDF).

Acknowledgements

We thank Q. Pang for help in the XRD experiment. Funding for this work is from the Natural Sciences and Engineering Research Council of Canada (NSERC).

References

- (1) Wang, Z. L. Nanostructures of Zinc Oxide. *Mater. Today* **2004**, *7*, 26-33.
- (2) Iyer, M. A.; Oza, G.; Velumani, S.; Maldonado, A.; Romero, J.; Muñoz, M. d. L.; Sridharan, M.; Asomoza, R.; Yi, J. Scanning Fluorescence-Based Ultrasensitive Detection of Dengue Viral DNA on ZnO Thin Films. *Sens. Actuators, B* **2014**, *202*, 1338-1348.
- (3) Wang, C.; Huang, N.; Zhuang, H.; Jiang, X. Enhanced Performance of Nanocrystalline ZnO DNA Biosensor via Introducing Electrochemical Covalent Biolinkers. *ACS Appl. Mater. Interfaces* **2015**, *7*, 7605-12.
- (4) Djurišić, A. B.; Chen, X.; Leung, Y. H.; Man Ching Ng, A. ZnO Nanostructures: Growth, Properties and Applications. *J. Mater. Chem.* **2012**, *22*, 6526.
- (5) Rasmussen, J. W.; Martinez, E.; Louka, P.; Wingett, D. G. Zinc Oxide Nanoparticles for Selective Destruction of Tumor Cells and Potential for Drug Delivery Applications. *Expert Opin. Drug Delivery* **2010**, *7*, 1063-77.
- (6) Kumar, S. A.; Chen, S. M. Nanostructured Zinc Oxide Particles in Chemically Modified Electrodes for Biosensor Applications. *Anal. Lett.* **2008**, *41*, 141-158.
- (7) Zhang, J.; Wu, D.; Li, M.-F.; Feng, J. Multifunctional Mesoporous Silica Nanoparticles Based on Charge-Reversal Plug-Gate Nanovalves and Acid-Decomposable ZnO Quantum Dots for Intracellular Drug Delivery. *ACS Appl. Mater. Interfaces* **2015**.
- (8) Liu, J.; Cao, Z.; Lu, Y. Functional Nucleic Acid Sensors. *Chem. Rev.* **2009**, *109*, 1948-98.

- (9) Li, D.; Song, S.; Fan, C. Target-Responsive Structural Switching for Nucleic Acid-Based Sensors. *Acc. Chem. Res.* **2010**, *43*, 631-641.
- (10) Fang, X.; Tan, W. Aptamers Generated from Cell-Selex for Molecular Medicine: A Chemical Biology Approach. *Acc. Chem. Res.* **2010**, *43*, 48-57.
- (11) Willner, I.; Zayats, M. Electronic Aptamer-Based Sensors. *Angew. Chem., Int. Ed. Engl.* **2007**, *46*, 6408-18.
- (12) Du, Y.; Li, B.; Wang, E. "Fitting" Makes "Sensing" Simple: Label-Free Detection Strategies Based on Nucleic Acid Aptamers. *Acc. Chem. Res.* **2013**, *46*, 203-13.
- (13) Jones, M. R.; Seeman, N. C.; Mirkin, C. A. Programmable Materials and the Nature of the DNA Bond. *Science* **2015**, *347*.
- (14) Sharma, V.; Anderson, D.; Dhawan, A. Zinc Oxide Nanoparticles Induce Oxidative DNA Damage and ROS-Triggered Mitochondria Mediated Apoptosis in Human Liver Cells (HepG2). *Apoptosis* **2012**, *17*, 852-870.
- (15) Sharma, V.; Shukla, R. K.; Saxena, N.; Parmar, D.; Das, M.; Dhawan, A. DNA Damaging Potential of Zinc Oxide Nanoparticles in Human Epidermal Cells. *Toxicol. Lett.* **2009**, *185*, 211-218.
- (16) Singh, S. P.; Arya, S. K.; Pandey, P.; Malhotra, B. D.; Saha, S.; Sreenivas, K.; Gupta, V. Cholesterol Biosensor Based on RF Sputtered Zinc Oxide Nanoporous Thin Film. *Appl. Phys. Lett.* **2007**, *91*, 140-142.

- (17) Wahab, R.; Kim, Y.-S.; Hwang, I. H.; Shin, H.-S. A Non-Aqueous Synthesis, Characterization of Zinc Oxide Nanoparticles and Their Interaction with DNA. *Synth. Met.* **2009**, *159*, 2443-2452.
- (18) Li, N.; Gao, Y.; Hou, L.; Gao, F. DNA-Based Toolkit for Directed Synthesis of Zinc Oxide Nanoparticle Chains and Understanding the Quantum Size Effects in ZnO Nanocrystals. *J. Phys. Chem. C* **2011**, *115*, 25266-25272.
- (19) Bawazer, L. A.; Newman, A. M.; Gu, Q.; Ibish, A.; Arcila, M.; Cooper, J. B.; Meldrum, F. C.; Morse, D. E. Efficient Selection of Biomineralizing DNA Aptamers Using Deep Sequencing and Population Clustering. *ACS Nano* **2014**, *8*, 387-395.
- (20) Vallee, B. L.; Auld, D. S. Cocatalytic Zinc Motifs in Enzyme Catalysis. *Proc. Natl. Acad. Sci. U. S. A.* **1993**, *90*, 2715-2718.
- (21) Auld, D. S.; Kawaguchi, H.; Livingston, D. M.; Vallee, B. L. RNA-Dependent DNA Polymerase (Reverse Transcriptase) from Avian Myeloblastosis Virus: A Zinc Metalloenzyme. *Proc. Natl. Acad. Sci. U. S. A.* **1974**, *71*, 2091-2095.
- (22) Lu, Y. New Transition-Metal-Dependent DNazymes as Efficient Endonucleases and as Selective Metal Biosensors. *Chem. - Eur. J.* **2002**, *8*, 4588-96.
- (23) Joyce, G. F. Directed Evolution of Nucleic Acid Enzymes. *Annu. Rev. Biochem.* **2004**, *73*, 791-836.
- (24) Schlosser, K.; Li, Y. Biologically Inspired Synthetic Enzymes Made from DNA. *Chem.*

- Biol.* **2009**, *16*, 311-322.
- (25) Silverman, S. K. Deoxyribozymes: Selection Design and Serendipity in the Development of DNA Catalysts. *Acc. Chem. Res.* **2009**, *42*, 1521-31.
- (26) Li, J. In Vitro Selection and Characterization of a Highly Efficient Zn(II)-Dependent RNA-Cleaving Deoxyribozyme. *Nucleic Acids Res.* **2000**, *28*, 481-488.
- (27) Santoro, S. W.; Joyce, G. F.; Sakhivel, K.; Gramatikova, S.; Barbas, C. F. RNA Cleavage by a DNA Enzyme with Extended Chemical Functionality. *J. Am. Chem. Soc.* **2000**, *122*, 2433-2439.
- (28) Dokukin, V.; Silverman, S. K. Lanthanide Ions as Required Cofactors for DNA Catalysts. *Chem. Sci.* **2012**, *3*, 1707-1714.
- (29) Gu, H.; Furukawa, K.; Weinberg, Z.; Berenson, D. F.; Breaker, R. R. Small, Highly Active DNAs that Hydrolyze DNA. *J. Am. Chem. Soc.* **2013**, *135*, 9121-9129.
- (30) Cuenoud, B.; Szostak, J. W. A DNA Metalloenzyme with DNA Ligase Activity. *Nature* **1995**, *375*, 611-4.
- (31) Blok, L.; De Bruyn, P. L. The Ionic Double Layer at the ZnO Solution Interface. II. Composition Model of the Surface. *J. Colloid Interface Sci.* **1970**, *32*, 527-532.
- (32) Pagba, C.; Zordan, G.; Galoppini, E.; Piatnitski, E. L.; Hore, S.; Deshayes, K.; Piotrowiak, P. Hybrid Photoactive Assemblies: Electron Injection from Host–Guest Complexes into Semiconductor Nanoparticles. *J. Am. Chem. Soc.* **2004**, *126*, 9888-9889.

- (33) Zhang, X.; Servos, M. R.; Liu, J. Surface Science of DNA Adsorption onto Citrate-Capped Gold Nanoparticles. *Langmuir* **2012**, *28*, 3896-902.
- (34) Zhang, X.; Wang, F.; Liu, B.; Kelly, E. Y.; Servos, M. R.; Liu, J. Adsorption of DNA Oligonucleotides by Titanium Dioxide Nanoparticles. *Langmuir* **2014**, *30*, 839-45.
- (35) Liu, B.; Liu, J. DNA Adsorption by Indium Tin Oxide Nanoparticles. *Langmuir* **2015**, *31*, 371-7.
- (36) Liu, B.; Liu, J. DNA Adsorption by Magnetic Iron Oxide Nanoparticles and Its Application for Arsenate Detection. *Chem. Commun.* **2014**, *50*, 8568.
- (37) Pautler, R.; Kelly, E. Y.; Huang, P. J. J.; Cao, J.; Liu, B. W.; Liu, J. W. Attaching DNA to Nanoceria: Regulating Oxidase Activity and Fluorescence Quenching. *ACS Appl. Mater. Interfaces* **2013**, *5*, 6820-6825.
- (38) Wu, M.; Kempaiah, R.; Huang, P.-J. J.; Maheshwari, V.; Liu, J. Adsorption and Desorption of DNA on Graphene Oxide Studied by Fluorescently Labeled Oligonucleotides. *Langmuir* **2011**, *27*, 2731-8.
- (39) Yun, C. S.; Javier, A.; Jennings, T.; Fisher, M.; Hira, S.; Peterson, S.; Hopkins, B.; Reich, N. O.; Strouse, G. F. Nanometal Surface Energy Transfer in Optical Rulers, Breaking the Fret Barrier. *J. Am. Chem. Soc.* **2005**, *127*, 3115-9.
- (40) Huang, P.-J. J.; Liu, J. DNA-Length-Dependent Fluorescence Signaling on Graphene Oxide Surface. *Small* **2012**, *8*, 977-83.

- (41) Nakanishi, K.; Sakiyama, T.; Imamura, K. On the Adsorption of Proteins on Solid Surfaces, a Common but Very Complicated Phenomenon. *J. Biosci. Bioeng.* **2001**, *91*, 233-244.
- (42) Franklin, N. M.; Rogers, N. J.; Apte, S. C.; Batley, G. E.; Gadd, G. E.; Casey, P. S. Comparative Toxicity of Nanoparticulate ZnO, Bulk ZnO, and ZnCl₂ to a Freshwater Microalga (*Pseudokirchneriella Subcapitata*): The Importance of Particle Solubility. *Environ. Sci. Technol.* **2007**, *41*, 8484-8490.
- (43) Soroka, K.; Vithanage, R. S.; Phillips, D. A.; Walker, B.; Dasgupta, P. K. Fluorescence Properties of Metal Complexes of 8-Hydroxyquinoline-5-Sulfonic Acid and Chromatographic Applications. *Anal. Chem.* **1987**, *59*, 629-636.
- (44) Saha, S.; Sarkar, P. Understanding the Interaction of DNA-RNA Nucleobases with Different ZnO Nanomaterials. *Phys. Chem. Chem. Phys.* **2014**, *16*, 15355-66.
- (45) Kemlo, J. A.; Shepherd, T. M. Quenching of Excited Singlet States by Metal Ions. *Chem. Phys. Lett.* **1977**, *47*, 158-162.
- (46) Varnes, A. W.; Dodson, R. B.; Wehry, E. L. Interactions of Transition-Metal Ions with Photoexcited States of Flavines. Fluorescence Quenching Studies. *J. Am. Chem. Soc.* **1972**, *94*, 946-950.
- (47) Fabbrizzi, L.; Licchelli, M.; Pallavicini, P.; Perotti, A.; Taglietti, A.; Sacchi, D. Fluorescent Sensors for Transition Metals Based on Electron-Transfer and Energy-Transfer Mechanisms. *Chem. - Eur. J.* **1996**, *2*, 75-82.

- (48) Spring, B. Q.; Clegg, R. M. Fluorescence Measurements of Duplex DNA Oligomers under Conditions Conducive for Forming M-DNA (a Metal-DNA Complex). *J. Phys. Chem. B* **2007**, *111*, 10040-52.
- (49) Santoro, S. W.; Joyce, G. F. A General Purpose RNA-Cleaving DNA Enzyme. *Proc. Natl. Acad. Sci. U. S. A.* **1997**, *94*, 4262-4266.
- (50) Liu, J.; Brown, A. K.; Meng, X.; Cropek, D. M.; Istok, J. D.; Watson, D. B.; Lu, Y. A Catalytic Beacon Sensor for Uranium with Parts-Per-Trillion Sensitivity and Millionfold Selectivity. *Proc. Natl. Acad. Sci. U. S. A.* **2007**, *104*, 2056-61.
- (51) Brown, A. K.; Li, J.; Pavot, C. M.-B.; Lu, Y. A Lead-Dependent DNzyme with a Two-Step Mechanism. *Biochemistry* **2003**, *42*, 7152-61.
- (52) Huang, P. J. J.; Lin, J.; Cao, J.; Vazin, M.; Liu, J. Ultrasensitive DNzyme Beacon for Lanthanides and Metal Speciation. *Anal. Chem.* **2014**, *86*, 1816-1821.